Supporting Information

Graphene Quantum Dots Sensitized Zn-MOF for Efficient Visible-Light-Driven Carbon Dioxide Reduction

Ding Wei,*[a] Wang Tang,[a] Yundan Gan[a] and Xiqing Xu*[b]

[a]Xi'an Modern Chemistry Research Institute, Xi'an, Shanxi 710061, P. R. China.

[b]School of Materials Science & Engineering, Chang'an University, Xi'an, Shanxi 710061, P. R. China.

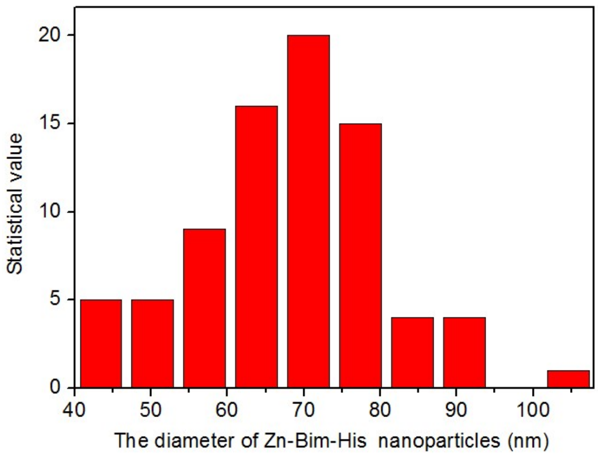

Figure S1. Statistical diameter for the synthesized Zn-Bim-His-1 nanoparticles.

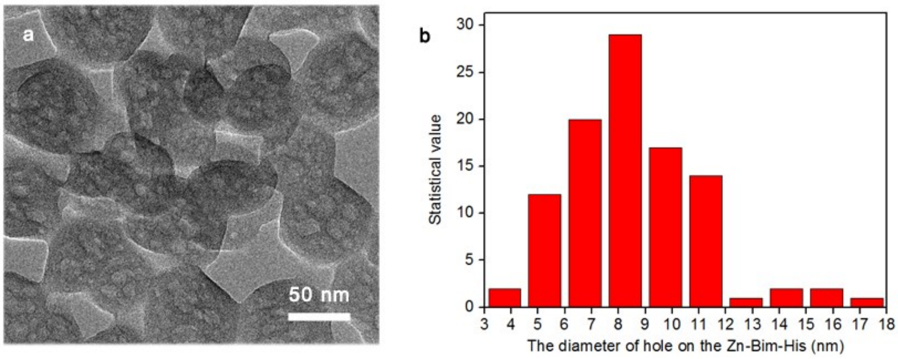

Figure S2. Statistical diameter for the hole on the surface of Zn-Bim-His-1 nanoparticles.

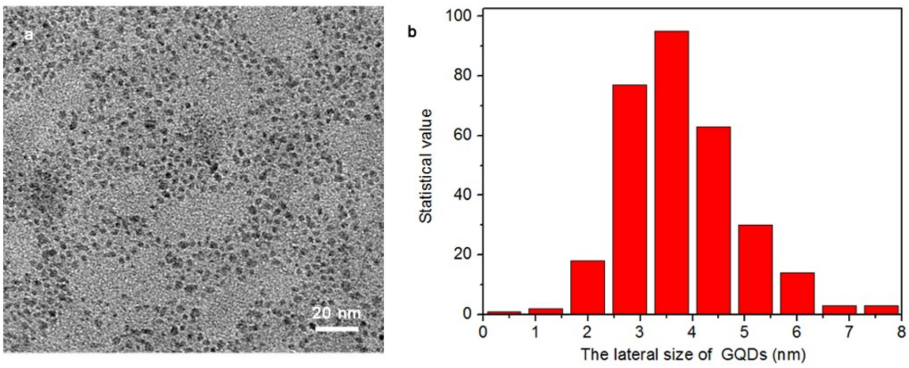

Figure S3. Statistical lateral size for GQDs.

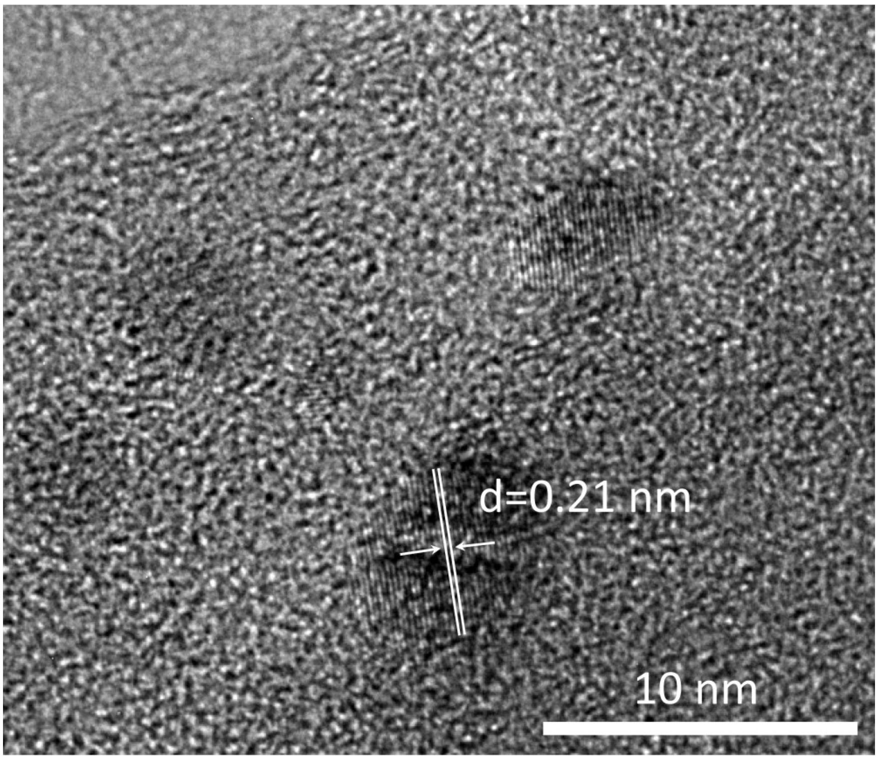

Figure S4. HRTEM image of Zn-Bim-His-1@GQDs in higher resolution.

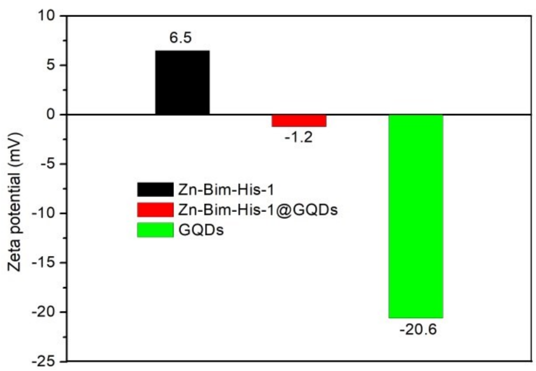

Figure S5. Histogram of the zeta potential value of Zn-Bim-His-1, GQDs and Zn-Bim-His-1@GQDs.

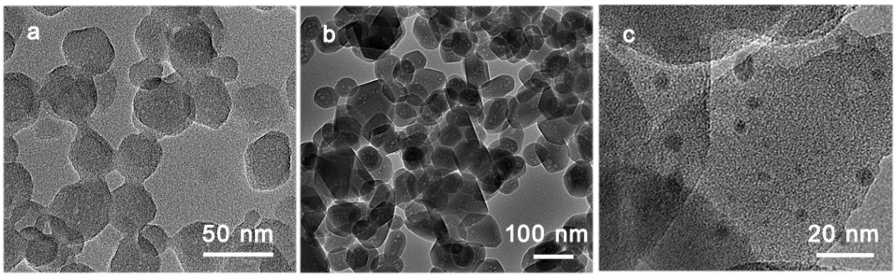

Figure S6. TEM of Zn-Bim@GQDs (a), Zn-Bim-His-2 (b) and Zn-Bim-His-2@ GQDs (c).

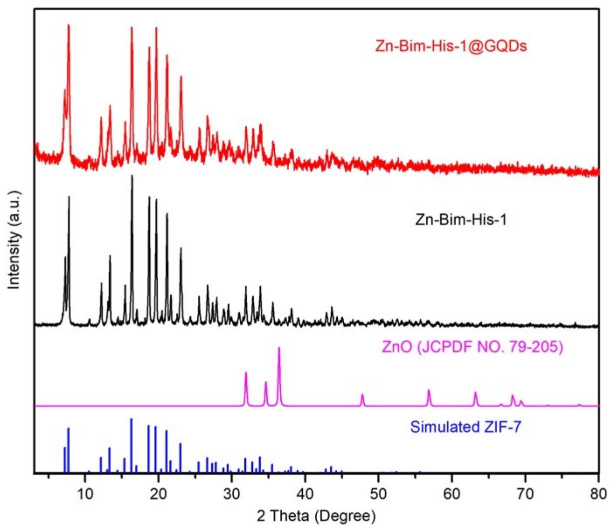

Figure S7. PXRD patterns of Zn-Bim-His-1, Zn-Bim-His-1@GQDs, pure ZnO (JCPDF NO. 79-205) and that simulated from crystal structure data for ZIF-7.[S1] The result shows the absence of impurities such as ZnO from the as prepared samples.

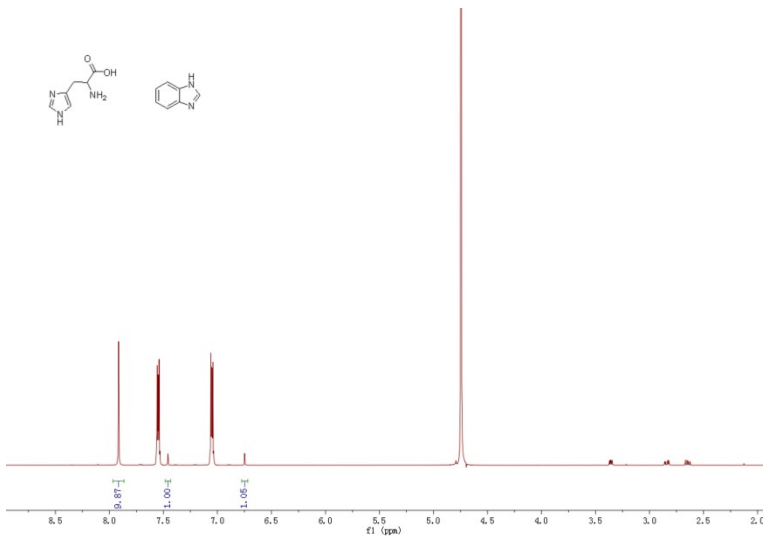

Figure S8. ^{1}H-NMR spectra for the Zn-Bim-His-1 sample. For ^{1}H-NMR analysis, the solution was prepared by digesting 20 mg of Zn-Bim-His-1 sample in NaOH (1 M)-D_2O solution for 24 h.

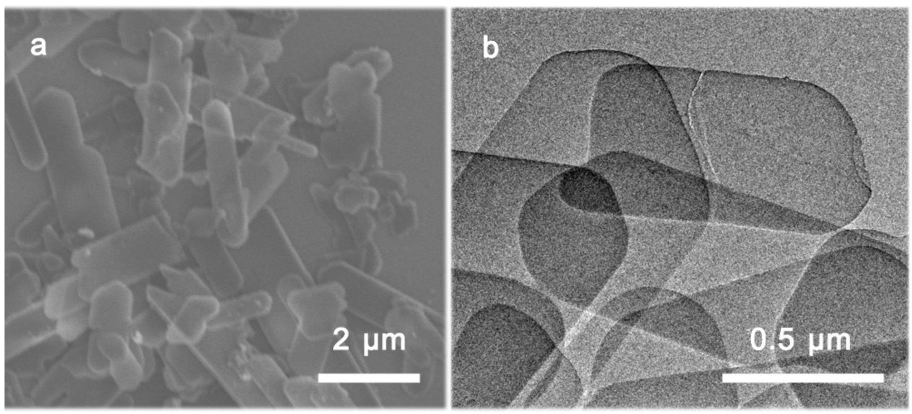

Figure S9. SEM and TEM of Zn-Bim-NH_2.

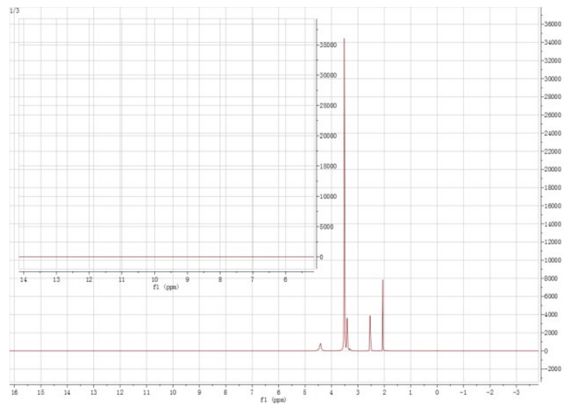

Figure S10. ^{1}H NMR spectra for the supernatant taken from the Zn-Bim-His-1@GQDs photocatalytic reaction system under visible light irradiation for 12 h.

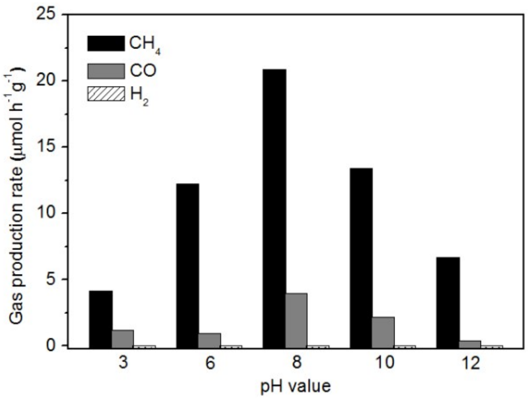

Figure S11. Product distribution during the photocatalytic CO_2 reduction using Zn-Bim-His-1@GQDs preparing in different pH values.

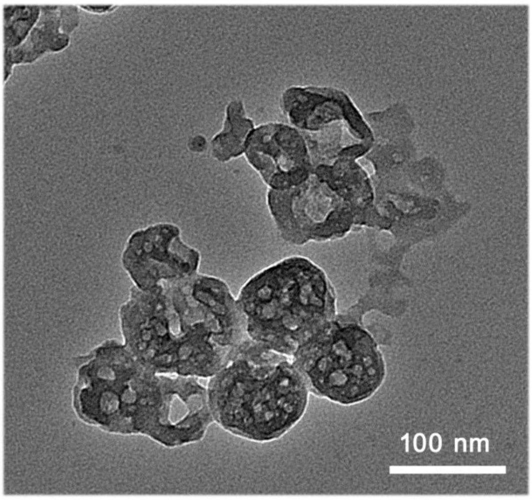

Figure S12. TEM of Zn-Bim-His-1@GQDs prepared under pH3.

Table S1. Comparison of photocatalytic performance for reduction of CO_2 with carbon dots catalyst and some noble-metal-containing systems reported in literature.

Catalyst	Light source	Sacrificial agent	Major product evolution rate μmol h^{-1} g^{-1}	Reference
Zn-Bim-His-1@GQDs	420＜λ＜750 nm	TEOA	CH_4: 20.9	This work
gold-doped carbon dots	405＜λ＜720 nm	--	$HCOO^-$: 8.5 ppm	S2
GQD-BNPTL	420＜λ＜800 nm	--	CH_3OH: 0.7	S3
CQDs/Cu_2O	λ＞400 nm	--	C_2H_6: 16.9	S4
$ZrOCo^{II}$/IrOx/ SBA-15 silica	355 nm	--	CO: 1.7	S5
ZnCr-LDH@Pt	UV	--	CO: 7.6	S6
C_3N_4/MgAl-LDH/Pd	500 W Hg(Xe) lamp without filter	--	CH_4: 0.8	S7
RuRu′/NS-C_3N_4, Ag	λ＞400 nm	EDTA·2Na	$COOH^-$: 57.5	S8
Pd-TiO_2	λ＞310 nm	--	CO: 0.4	S9
Cu_2S/Pt NR	450 W Xe lamp with a cutoff water filter for the IR wavelengths	Na_2SO_3	CO: 3.0	S10
Pt-g-C_3N_4/$NaNbO_3$	λ＞420 nm	--	CH_4: 6.4	S11
Pt/SiC	simulated sunlight	--	CH_4: 13.6	S12
PbS/TiO_2	420＜λ＜610 nm	--	CO: 0.8	S13
Cu/Pt/TiO_2	320＜λ＜780 nm	--	CH_4: 33.0	S14
rGO/$NiWO_4$@Au	simulated sunlight	--	CO: 0.9	S15

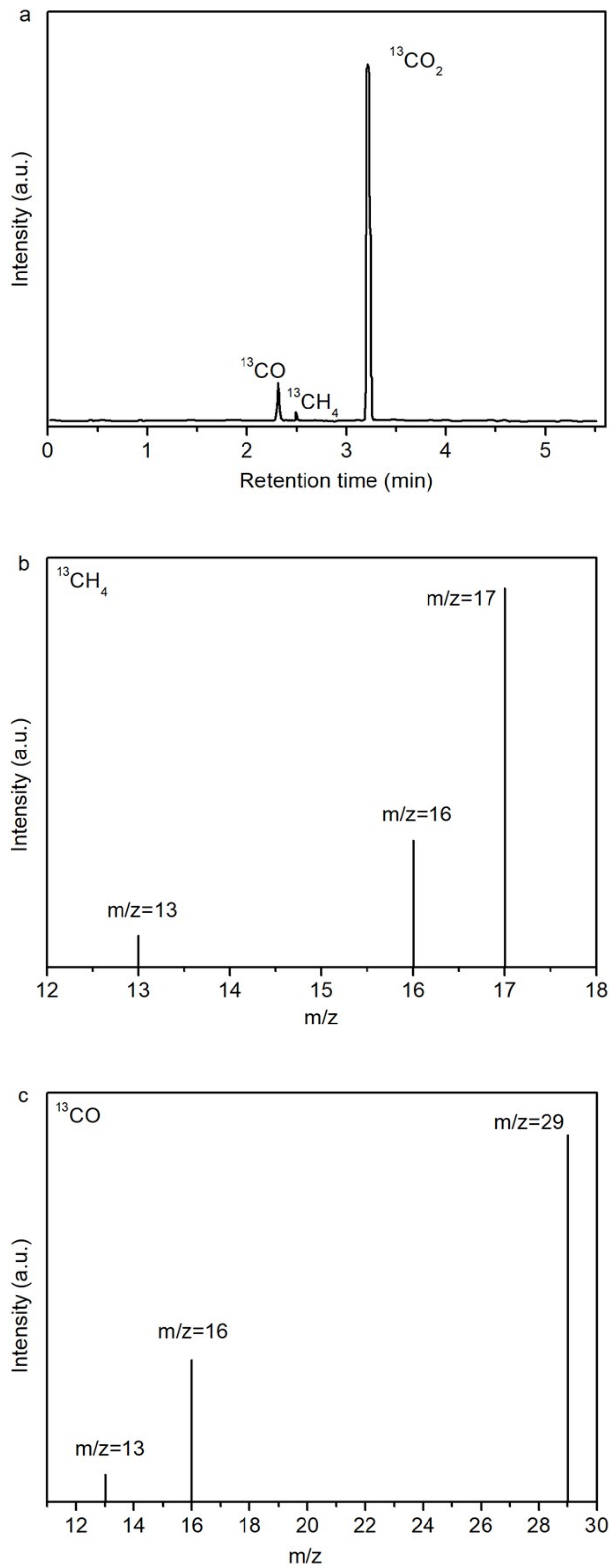

Figure S13. GC-MS spectras of the products generated from the $^{13}CO_2$ isotope experiments. (a) GC spectrum, (b, c) mass spectra showing $^{13}CH_4$ (m/z = 17) and ^{13}CO (m/z = 29) produced over Zn-Bim-His-1@GQDs.

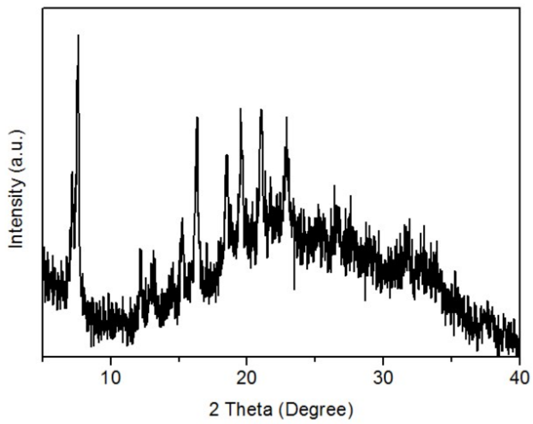

Figure S14. XRD patterns for Zn-Bim-His-1@GQDs hybrid nanoparticles after 48 h photocatalytic test.

References

S1 K. S. Park, Z. Ni, A. P. Côt´ e, J. Y. Choi, R. Huang, F. J. Uribe-Romo, H. K. Chae, M. O'Keeffe and O. M. Yaghi, *Proc. Natl. Acad. Sci. U. S. A.*, 2006, **103**, 10186-10191.

S2 S. Sahu, Y. Liu, P. Wang, C. E. Bunker, K. A. S. Fernando, W. K. Lewis, E. A. Guliants, F. Yang, J. Wang and Y. P. Sun, *Langmuir*, 2014, **30**, 8631-8636.

S3 Y. Yan, J. Chen, N. Li, J. Tian, K. Li, J. Jiang, J. Liu, Q. Tian and P. Chen, *ACS Nano*, 2018, **12**, 3523-3532.

S4 T. Kulandaivalu, S. Abdul Rashid, N. Sabli and T. L. Tan, *Diamond Relat. Mater.*, 2019, **91**, 64-73.

S5 W. Kim, G. Yuan, B. A. McClure and H. Frei, *J. Am. Chem. Soc.*, 2014, **136**, 11034-11042.

S6 K. I. Katsumata, K. Sakai, K. Ikeda, G. Carja, N. Matsushita and K. Okada, *Mater. Lett.*, 2013, **107**, 138-140.

S7 J. Hong, W. Zhang, Y. Wang, T. Zhou and R. Xu, *ChemCatChem*, 2014, **6**, 2315-2321.

S8 R. Kuriki, M. Yamamoto, K. Higuchi, Y. Yamamoto, M. Akatsuka, D. Lu, S. Yagi, T. Yoshida, O. Ishitani and K. Maeda, *Angew. Chem. Int. Ed.*, 2017, **56**, 4867-4871.

S9 T. Yui, A. Kan, C. Saitoh, K. Koike, T. Ibusuki and O. Ishitani, *ACS Appl. Mater. Inter.*, 2011, **3**, 2594-2600.

S10 A. Manzi, T. Simon, C. Sonnleitner, M. Döblinger, R. Wyrwich, O. Stern, J. K. Stolarczyk and J. Feldmann, *J. Am. Chem. Soc.*, 2015, **137**, 14007-14010.

S11 H. Shi, G. Chen, C. Zhang and Z. Zou, *ACS Catal.*, 2014, **4**, 3637-3643.

S12 C. Han, B. Wang, N. Wu, S. Shen and Y. Wang, *Appl. Surf. Sci.*, 2020, **515**, 145952.

S13 C. Wang, R. L. Thompson, P. Ohodnicki, J. Baltrus and C. Matranga, *J. Mater. Chem.*, 2011, **21**, 13452-13457.

S14 Q. Zhai, S. Xie, W. Fan, Q. Zhang, Y. Wang, W. Deng and Y. Wang, *Angew. Chem. Int. Ed.*, 2013, **52**, 5776-5779.

S15 J. Shin, J. N. Heo, J. Y. Do, Y. I. Kim, S. J. Yoon, Y. S. Kim and M. Kang, *J. Ind. Eng. Chem.*, 2020, **81**, 427-439.